Available online at www.sciencedirect.com
SCIENCE DIRECT
Bioorganic & Medicinal Chemistry 14 (2006) 2487–2497
Bioorganic & Medicinal Chemistry

Sesquiterpene lactones as inhibitors of IL-8 expression in HeLa cells

Maja T. Lindenmeyer,[a] Andrea Hrenn,[a] Claudia Kern,[a] Victor Castro,[b] Renato Murillo,[b] Stefan Müller,[a] Stefan Laufer,[c] Jürgen Schulte-Mönting,[d] Bettina Siedle[a] and Irmgard Merfort[a,*]

[a]*Institute of Pharmaceutical Science, Department of Pharmaceutical Biology and Biotechnology, University of Freiburg, 79104 Freiburg, Germany*
[b]*Escuela de Quimica and CIPRONA, Universidad de Costa Rica, San José, Costa Rica*
[c]*Institute of Pharmacy, University of Tübingen, Germany*
[d]*Institute of Medical Biometry and Medicinal Informatics, University of Freiburg, Germany*

Received 15 August 2005; revised 10 November 2005; accepted 15 November 2005
Available online 1 December 2005

Abstract—Twenty-four structurally different SLs were studied for their inhibition on IL-8 production in HeLa229 cells and different IC_{50}-values were obtained. QSAR analyses revealed that the α-methylene-γ-lactone and the presence and reactivity of a second reaction center, expressed by LUMO2, are the most important descriptors for IL-8. Using two SLs as examples, we demonstrated that SLs prevent DNA binding of AP-1, which has binding sites in the IL-8 promoter together with NF-κB and C/EBP, and that this is probably due to directly targeting AP-1. p38 MAPK, which plays a role in AP-1 activation as well as in IL-8 regulation, was not influenced by SLs. These data show that NF-κB and AP-1, and consequently IL-8 may be interesting targets in antiinflammation research and that the small molecules of SLs may be powerful candidates with promising properties for therapeutic modulation of the inflammatory response.

1. Introduction

Inflammation is a host response to a wide variety of tissue injuries characterized by the recruitment of leukocytes from the blood to the injured tissue. This movement is directed by chemokines among which interleukin-8 (IL-8) plays an important role. This multifunctional CXC chemokine possesses a wide range of potent stimulatory effects on neutrophils in vitro, including chemotaxis, degranulation of degrading enzymes, formation of bioactive lipids, integrin upregulation, expression of adhesion molecules on neutrophils, transendothelial migration, and cytoplasmatic Ca^{2+} elevation.[1,2] Its production is rapidly induced by proinflammatory stimuli, such as cytokines (e.g., tumor necrosis factor-α (TNF-α)), reactive oxidants, cellular stress, bacterial products, and viruses.[2] These stimuli coordinately activate distinct types of transcription factors in a highly cell type specific manner and induce IL-8 expression. The IL-8 promoter contains binding sites for a nuclear factor-κB (NF-κB) element that is required for activation in all cell types studied.[3,4] NF-κB is a dimeric transcription factor formed by the hetero- or homodimerization of proteins from the rel-family.[5] The mammalian rel-family consists of five members, namely Rel (c-Rel), p65 (Rel A), Rel B, p50, and p52, from which preferentially Rel p65/p65 homodimers as well as some p50/p65 heterodimers are bound to the IL-8 promoter.[6] The core IL-8 promoter also contains activator protein-1 (AP-1) and CAAT/enhancer-binding protein (C/EBP)-binding sites. Both binding sites are not essential for induction but are required for maximal expression.[3] AP-1 is an inducible transcription factor that is composed of either Jun–Fos heterodimers or Jun–Jun homodimers.[7] Besides the transcriptional control of IL-8 production, a regulation at the post-transcriptional level could be shown. Several reports indicate that after stimulation activation of the p38 MAPK pathway stabilizes the IL-8 mRNA via its downstream effector molecule MK-2 (MAPK-activated protein-2).[3,8] Collectively, these

Keywords: Sesquiterpene lactones; Interleukin-8; QSAR; Antiinflammatory activity; NFκB; AP-1.
* Corresponding author. Tel.: +49 761 203 8373; fax: +49 761 203 8383; e-mail: irmgard.merfort@pharmazie.uni-freiburg.de

0968-0896/$ - see front matter © 2005 Elsevier Ltd. All rights reserved.
doi:10.1016/j.bmc.2005.11.027

observations suggest that therapeutic targeting of the production of IL-8 may effectively be achieved by inhibiting the above-mentioned key intracellular signaling molecules.

Previously, we and others have shown that sesquiterpene lactones being the active constituents of many medicinal plants from the Asteraceae family are potent inhibitors of the transcription factor NF-κB.[9–13] We have also carried out quantitative structure–activity relationship (QSAR) studies on their NF-κB inhibiting properties using concentrations which completely inhibited DNA binding and which were named as IC_{100}-values.[9] Furthermore, Mazor et al. have already demonstrated that pretreatment with isohelenin or parthenolide inhibited TNF-α mediated IL-8 gene expression in cultured human respiratory epithelium.[12]

To enlarge our knowledge on structural features which may be related to the inhibitory activity, we investigated 24 structurally different SLs for their effect on IL-8 production in HeLa229 cells and carried out QSAR calculations with the more precise IC_{50}-values. The selected SLs represent all major skeletal classes, including germacranolides with the subtype germacrolides, furanoheliangolides and melampolides, eudesmanolides, guaianolides, and pseudoguaianolides. These compounds differ from each other in their molecular geometry and in the number of α,β-unsaturated carbonyl structure elements. We compared the activity of SLs in the IL-8 ELISA with that found in the NF-κB EMSA in which the influence on NF-κB DNA binding is studied. Furthermore, we studied whether inhibition of the transcription factor AP-1 and of the p38 MAP kinase is involved in downregulation of IL-8-expression by SLs besides the already proven inhibition of the transcription factor NF-κB.

2. Results and discussion

2.1. Effects of sesquiterpene lactones on IL-8 production in HeLa229 cells and quantitative structure–activity relationships

SLs **1**–**24** (for structures, see Fig. 1, for names and references, see Table 2) were investigated for their effect on TNF-α mediated production of immunoreactive IL-8. HeLa229 cells were preincubated with the respective SLs at various concentrations for 1 h and subsequently stimulated with TNF-α (800 U/ml) for 24 h. Supernatants were collected and the amount of IL-8 secretion was determined in an ELISA. Dexamethasone was used as a standard. Cell viability was greater than 85% after 24 h exposure to the experimental conditions (data not shown). For SL **8** a cell viability of only 70% was measured. Figure 2 exemplarily shows the dose–dependent curves for six structurally different SLs representing all major skeletal classes. Depending on the structural

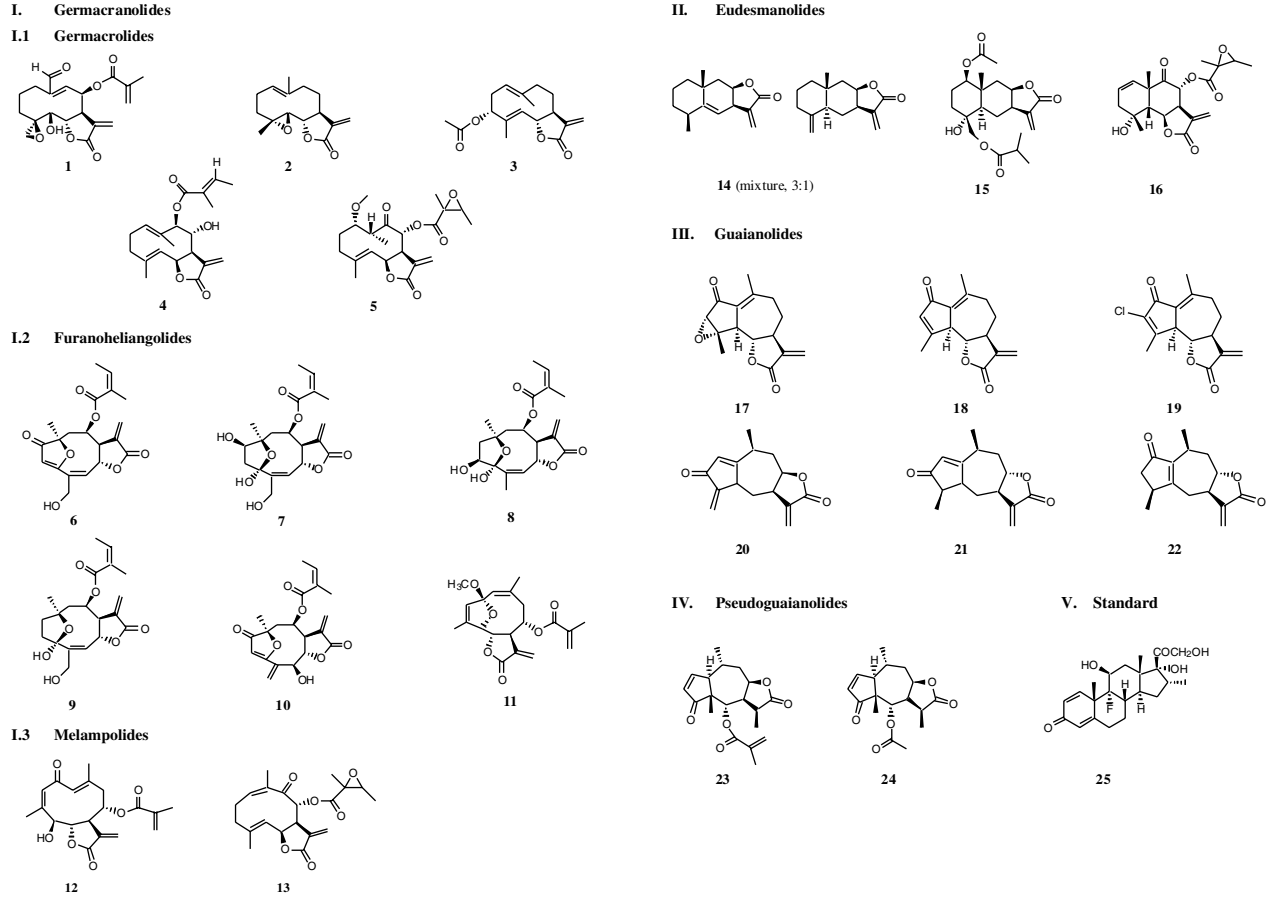

Figure 1. Structures of the investigated sesquiterpene lactones.

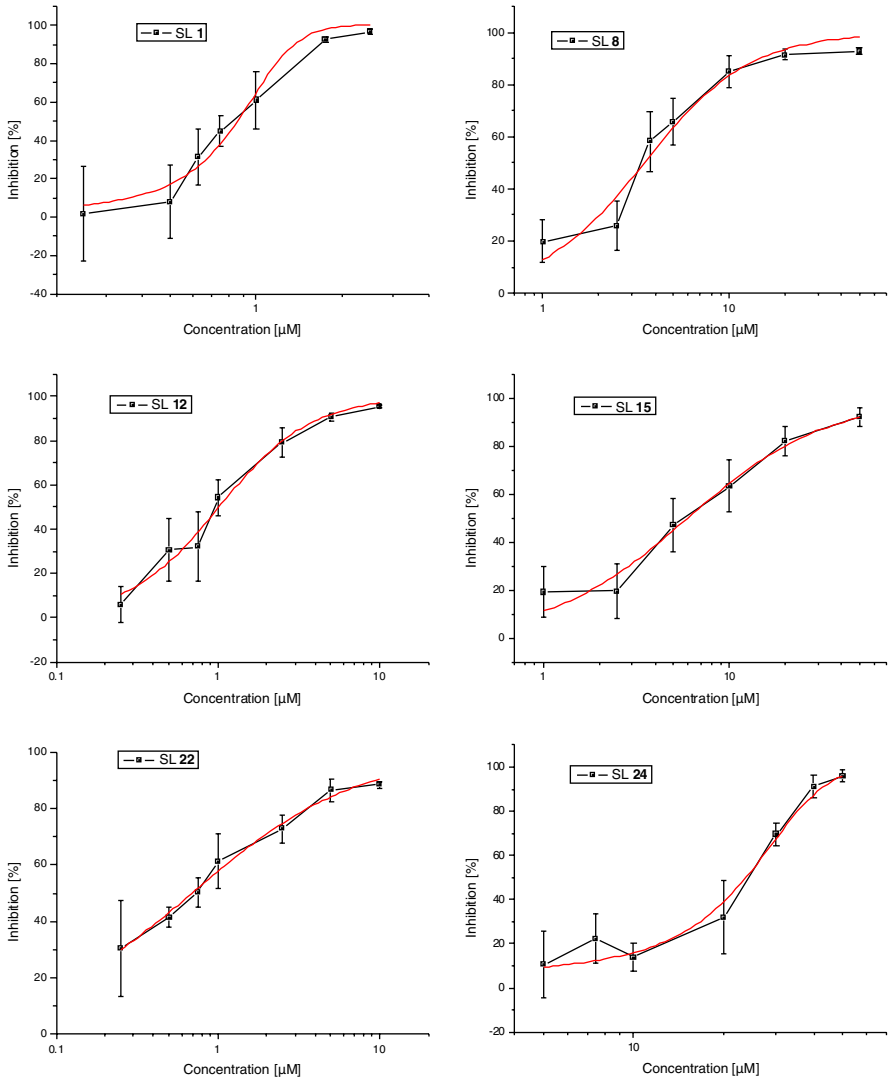

Figure 2. ELISA results as dose–response curves demonstrating exemplarily the effects of SLs **1**, **8**, **12**, **15**, **22**, and **24** on TNF-α-mediated production of IL-8 in HeLa229 cells. HeLa229 cells were pretreated with indicated concentrations of the SL for 1 h before being incubated with TNF-α (800 U/ml) for 24 h. Cells were lysed and analyzed for IL-8 production as described in the Experimental. Each point shows the means ± SD of at least two independent experiments carried out in triplicate.

features different IC_{50}-values were obtained (Table 1). IC_{50}-values correlated quite well with the concentrations needed for complete inhibition of the transcription factor NF-κB (see Table 1). Those SLs from which only low concentrations were necessary for a complete inhibition of NF-κB DNA binding were also the most active compounds in inhibiting IL-8 production. However, the IC_{50}-values were much lower than the concentrations needed for complete inhibition of NF-κB DNA binding. This may be explained by the fact that SLs influence further participating signaling pathways or further transcription factors in the promoter region of the IL-8 gene. It can also be due to the different incubation times used in the EMSA (2 h) and in the ELISA (24 h).

To study the structural features responsible for the inhibition activity on IL-8 production and NF-κB DNA binding in these series of structural different SLs, we analyzed the influence of different descriptors on the IC_{50}-values of IL-8 and the IC_{100}-values of NF-κB. The latter values were taken either from previous investigations or, in the case of SLs **6**–**10** determined during these studies. A 3D-structure was created for all the investigated SLs using the HYPERCHEM® program. The low-energy conformations were semi-empirically minimized using the AM1 algorithm and transferred into the CAChe® database. Using the two-step model selection procedure (described in Section 4) an equation with two variables proved to be the best to describe the correlation between the inhibition of IL-8 production (IC_{50}—IL-8, Eq. 1) as well as of NF-κB DNA binding activity (IC_{100}—NF-κB, Eq. 2) and the physico-chemical properties of the molecules. The following two equations were obtained:

$$\begin{aligned} pIC_{50} &= 0.694(\pm 0.194)ML \\ &\quad - 0.505(\pm 0.128)LUMO2 \\ &\quad - 0.825(\pm 0.191) \end{aligned} \tag{1}$$

Table 1. Experimental and calculated IC_{50} values (μM) obtained in the IL-8 ELISA using HeLa229 cells and concentrations necessary for complete inhibition of NF-κB DNA binding, named as IC_{100} (μM) using Jurkat T-cells

Sl no.	IL-8				NF-κB			
	IC_{50} exp	IC_{50} calcd	pIC_{50} exp	pIC_{50} calcd	IC_{100} exp	IC_{100} calcd	pIC_{100} exp	pIC_{100} calcd
1	0.86 (±0.04)	0.95	0.066	0.023	5	13.08	−0.699	−1.117
2	2.38 (±0.31)	3.16	−0.377	−0.500	20	40.11	−1.301	−1.603
3	2.89 (±0.18)	2.64	−0.461	−0.422	50	33.95	−1.699	−1.531
4	1.31 (±0.20)	1.98	−0.117	−0.297	50	25.99	−1.699	−1.415
5	1.30 (±0.19)	2.15	−0.114	−0.332	20	27.97	−1.301	−1.447
6	0.84 (±0.11)	1.10	0.076	−0.040	5	14.96	−0.699	−1.175
7	2.20 (±0.32)	1.34	−0.342	−0.129	20	18.10	−1.301	−1.258
8	3.49 (±0.36)	1.32	−0.543	−0.121	50	17.79	−1.699	−1.250
9	1.85 (±0.15)	1.30	−0.267	−0.115	20	17.58	−1.301	−1.245
10	1.23 (±0.18)	1.15	−0.090	−0.061	10	15.66	−1.301	−1.195
11	1.04 (±0.15)	1.21	−0.017	−0.083	10	16.42	−1	−1.215
12	1.01 (±0.07)	0.93	−0.004	−0.030	10	12.90	−1	−1.111
13	2.92 (±0.29)	1.36	−0.465	−0.133	50	18.26	−1.699	−1.262
14	4.81 (±0.46)	3.42	−0.682	−0.534	100	43.17	−2	−1.635
15	5.98 (±0.66)	3.90	−0.777	−0.591	100	48.79	−2	−1.689
16	1.78 (±0.17)	2.30	−0.250	−0.363	10	29.88	−1	−1.475
17	0.39 (±0.04)	0.97	0.409	0.012	5	13.38	−0.699	−1.127
18	2.79 (±0.23)	1.03	−0.446	−0.012	50	14.11	−1.699	−1.150
19	1.64 (±0.18)	0.96	−0.212	0.018	20	13.23	−1.301	−1.121
20	0.66 (±0.07)	1.69	0.180	−0.229	10	22.45	−1	−1.351
21	0.46 (±0.06)	1.01	0.338	−0.005	20	13.89	−1.301	−1.143
22	0.69 (±0.04)	1.13	0.161	−0.051	20	15.34	−1.301	−1.186
23	7.94 (±0.82)	7.65	−0.900	−0.883	100	82.00	−2	−1.914
24	23.75 (±1.24)	24.67	−1.376	−1.392	200	243.89	−2.301	−2.387
25	0.0008 (±0.0002)				nd			

Calculations were obtained by Eq. 1 for IL-8 and Eq. 2 for NF-κB. IC_{50} values of IL-8 inhibition were calculated using the non-linear fitting option of the program ORIGIN 7.0.

$$n = 24, \quad R = 0.821, \quad R^2 = 0.6742, \quad s = 0.246,$$
$$F = 21.728, \quad P > 0.0001$$

$$\begin{aligned} pIC_{100} = {} & 0.599(\pm 0.250)\mathrm{ML} \\ & - 0.470(\pm 0.164)\mathrm{LUMO2} \\ & - 1.859(\pm 0.246) \end{aligned} \tag{2}$$

$$n = 24, \quad R = 0.709, \quad R^2 = 0.5028, \quad s = 0.317,$$
$$F = 10.617, \quad P > 0.0007$$

The most important variable for both biological activities turned out to be the α-methylene-γ-lactone moiety which has been already described as a significant feature for various biological activities including the NF-κB inhibitory activity.[9,14–16] The importance of this parameter has also been demonstrated for other biological activities, such as the antiinflammatory activity, proven in vivo, and cytotoxicity.[14,16] LUMO2 is the next important criterion. It quantifies the energy necessary to remove an electron from the second lowest unoccupied molecular orbital and corresponds to the reactivity of the second reaction center of the molecule, which is either the α-methylene-γ-lactone moiety or another α,β-unsaturated carbonyl function. Interestingly, considering the correlation factors for NF-κB ($R = 0.709$) and IL-8 ($R = 0.821$) a slight improvement using the IC_{50} values has been achieved. As expected from the correlation coefficient deviations are observed between the experimental and predicted IC_{100}-values for inhibition of NF-κB DNA binding (see Table 1 and Fig. 3 right).

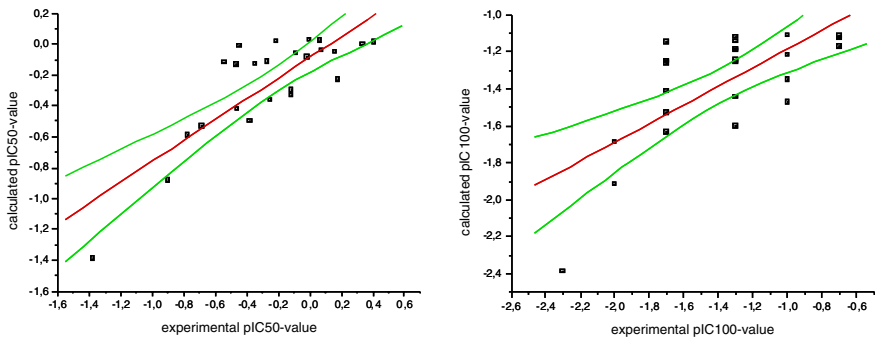

Figure 3. Regression model of Eq. 1 (left, IL-8) and Eq. 2 (right, NF-κB) derived from all 24 SLs. Data points, regression line, and 95% confidence interval (pointed).

2.2. SLs inhibit NF-κB DNA binding activity with different concentrations in Jurkat T-cells and HeLa cells

As the IC_{50}-values for inhibition of the IL-8 production in HeLa cells were much lower than expected from the NF-κB data which were obtained in Jurkat T-cells, we tested, whether this phenomenon may be related to the different cell lines. SLs from *Viguiera sylvatica* were used exemplarily. Jurkat T-cells and HeLa cells were incubated with the respective SLs at various concentrations for 1 h and subsequently stimulated with TNF-α (200 U/ml) for one further hour. Total protein extracts were prepared and analyzed for NF-κB DNA binding activity in an EMSA (Figs. 4A–C). Compound **6** completely inhibited activation of NF-κB at a concentration of 5 μM in Jurkat T-cells, while in HeLa cells a complete inhibition was observed at 20 μM. A similar observation was obtained for compounds **7** and **9**, from which lower concentrations were needed for complete inhibition (20 μM) in Jurkat T-cells than in HeLa cells (50 μM). However, compounds **8** and **10** inhibited NF-κB DNA binding in both cell lines at the same concentration (SL **8**: 50 μM; SL **10**: 10 μM). The slight differences in inhibitory activity toward HeLa as well as Jurkat T-cells may be due to the different glutathione levels. It has already been found that increasing concentrations of glutathione overcome the inhibitory effects of thiol-reactive drugs like cisplatin or D-penicillamines.[17] SLs are also known to efficiently form adducts with glutathione.[18] Nevertheless, despite the observed differences in activity these results cannot explain the discrepancy in the IC_{50} values of IL-8 inhibition and in the IC_{100} values of NF-κB inhibition.

2.3. The SL parthenolide down-regulates IL-8 mRNA expression levels

Next, we investigated the impact of SLs on IL-8 mRNA expression in HeLa cells using parthenolide (**2**) as an

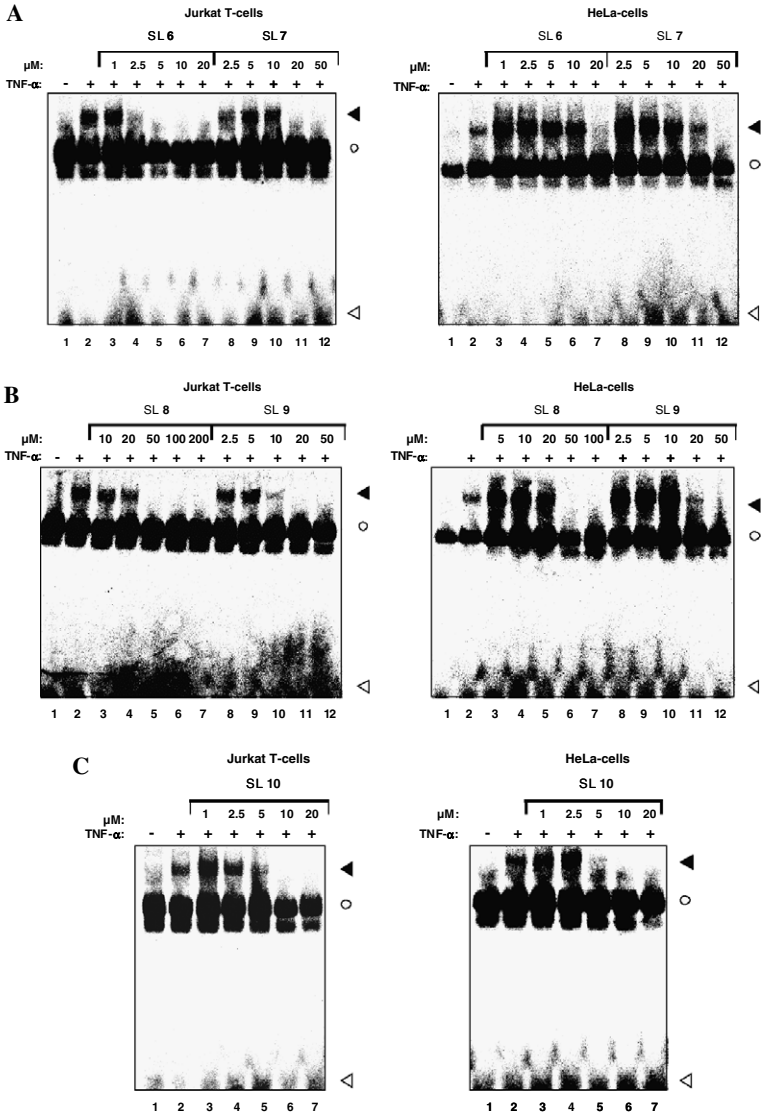

Figure 4. The effect of SLs **6**–**10** on NF-κB DNA binding in Jurkat T-cells or HeLa cells. In A–C lane 1 shows unstimulated control cells, in lane 2 cells were treated with 200 U/ml TNF-α alone. In lanes 3–10 (A and B) and 3–7 (C), cells were pretreated for 1 h with various concentrations of SLs **6**–**10** and subsequently stimulated with TNF-α for 1 h. A filled arrowhead indicates the position of NF-κB DNA complexes. The open circle denotes a non-specific activity binding to the probe. The open arrowhead shows unbound oligonucleotide.

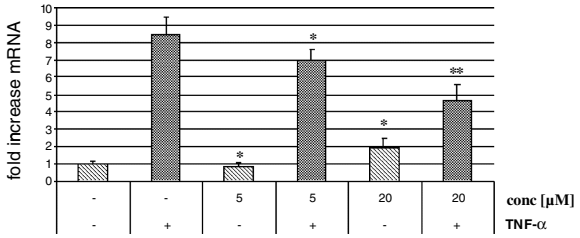

Figure 5. Parthenolide (**2**) inhibits IL-8 mRNA expression in HeLa 229 cells. Given is the fold increase in mRNA levels relative to cells untreated with parthenolide, respectively. HeLa cells were preincubated with different concentrations of parthenolide for 1 h and subsequently stimulated with TNF-α (2 ng/ml) for 7 h. Total RNA isolation was performed using RNeasy Mini Kit (Qiagen), reverse-transcribed in cDNA, and analyzed via quantitative real-time PCR (TaqMan®). Data represent means ± SEM of two separate experiments with each condition carried out in duplicate. $*p < 0.05$, $**p < 0.005$ versus the control being either without TNF-α or with TNF-α-stimulation, respectively.

example. This SL was chosen, because of its middle IL-8 inhibitory activity. Analysis by quantitative real-time PCR (Taqman®) showed that a 5 μM concentration of SL **2** had only a slight effect, whereas a 20 μM concentration decreased mRNA expression by about 50% (see Fig. 5). However, the low IC_{50}-values obtained in the IL-8 ELISA cannot be explained on the transcriptional level. Interestingly, treatment of HeLa cells with SL **2** alone resulted in a slight, but significant, increase in mRNA level.

2.4. SLs inhibit DNA binding of AP-1 in HeLa229-cells

IL-8 gene expression is regulated by a set of transcription factors, such as NF-κB and AP-1.[5,7] Whereas the inhibitory activity of SLs toward NF-κB DNA binding is well known, their behavior toward AP-1 is controversely discussed. On the one hand Bork et al.[19] showed that parthenolide and isohelenin (= isoalantolactone) did not influence DNA binding of AP-1 in HeLa cells, while on the other hand Kang et al.[20] proved for the germacranolide costunolide differing from parthenolide only in the stable epoxy ring that AP-1 DNA binding activity was downregulated in RAW 264.7 cells. We examined the effect of SLs on the activity of AP-1 using SLs **1** and **2** as representative examples. HeLa cells were treated with PMA (100 ng/ml) for 1 h after preincubation (1 h) with SL **1** or **2** at the specified concentrations. Nuclear protein extracts were prepared and analyzed for AP-1 DNA binding activity by EMSA (Fig. 6). Competition assay verified the presence of AP-1 (data not shown). SL **1** and **2** nearly completely inhibited activation of AP-1 at a concentration of 30 and 50 μM, respectively, without showing any cytotoxic effects. These data contradict observations of Bork et al.[19] but are in line with the above-mentioned results from Kang et al.[20]

SLs can react with biological nucleophiles, especially with the thiol group of cysteine, in a Michael-type addition,[18] as it was already shown by us for p65/NF-κB.[13] The possibility arises that they also directly modify the AP-1 DNA binding activity as it was proven for 15-de-

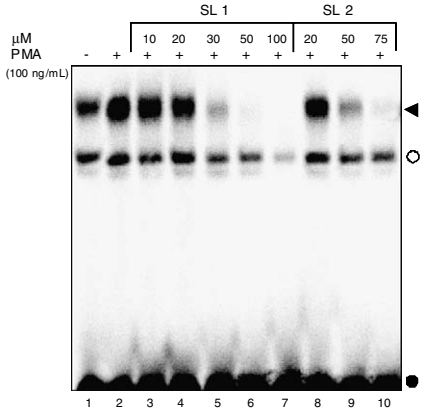

Figure 6. The effect of SLs **1** and **2** on AP-1 DNA binding in PMA-stimulated HeLa229 cells. Lane 1 shows unstimulated control cells; in lane 2, cells were treated with 100 ng/ml PMA alone for 1 h. Lanes 3–10 show cells pretreated for 1 h with the indicated concentrations of SL **1** or SL **2** and subsequently stimulated with 100 ng/ml PMA for 1 h. Nuclear extracts were prepared and analyzed by EMSA. A filled arrowhead indicates the position of AP-1 DNA complexes. The open circle denotes a non-specific activity binding to the probe. The filled circle shows unbound oligonucleotide.

oxy-$\Delta^{12,14}$-prostaglandin J_2 as well as for gold(I) and selenite.[21,22] Therefore, we investigated the effect of SL **2** on AP-1 DNA binding in PMA-pretreated HeLa cells. These cells were stimulated with PMA for 1 h and then incubated with various concentrations of SL **2** for 2 h. The extracts were analyzed for AP-1 DNA binding by EMSA. Figures 7A and B (lanes 7 and 9, respectively) show that compound **2** inhibits AP-1 DNA binding after it is already present in active form, but in contrast to the normal ex vivo experiment a higher concentration (75 μM) is necessary for a complete inhibition of AP-1 DNA binding (Figs. 7A and B, lane 7). From this result it can be assumed that SL **2** directly interferes with AP-1.

To prove that AP-1 inhibition is due to irreversible alkylation of free sulfhydryls on cysteine residues, the ex vivo experiment was modified. In a first experiment (Fig. 7A), an excess of the reducing agent DTT was added 1 h after PMA-stimulation and 10 min prior to SL **2** addition. If SL **2** modifies AP-1 by alkylation, an excess of DTT should prevent this reaction, since the SL would react with the large quantities of free sulfhydryls in the DTT instead of reacting with AP-1. Indeed, DTT completely suppressed the inhibitory effect of SL **2** at various concentrations on AP-1 DNA binding (Fig. 7A, lanes 6, 8, and 10). However, addition of DTT for 1 h after incubation with 75 and 100 μM concentrations of SL **2** had no effect on the inhibitory influence on AP-1 DNA binding (Fig. 7B, lanes 8 and 10).

These experiments carried out with DTT strongly indicated that SLs may alkylate critical residues present in the DNA binding domain of AP-1 proteins which are essential for DNA binding.[21,23] These cysteine residues are flanked by basic lysine and arginine favoring a Michael-type addition of cysteine's thiol group by SLs. This inhibition mechanism was already proven for

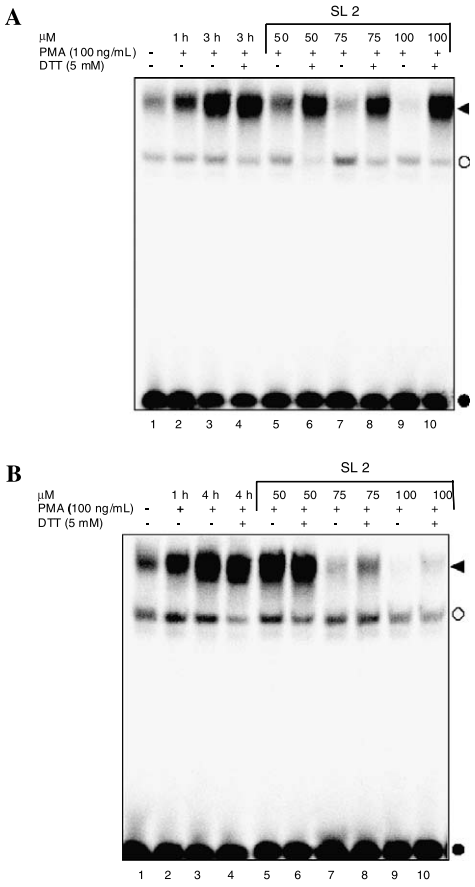

Figure 7. The effects of SL **2** on AP-1 DNA binding in the presence of DTT in HeLa229 cells. (A) The influence of SL **2** on AP-1 DNA binding after preincubation with DTT. Lane 1 shows unstimulated control cells. In lane 2, cells were treated with 100 ng/ml PMA alone for 1 h, in lane 3 for 3 h. In lanes 4, 6, 8, and 10, cells were stimulated with PMA. After 1 h DTT was added to a final concentration of 5 mM. Ten minutes after DTT addition, different concentrations of SL **2** were added and cells were incubated for further 2 h (lanes 6, 8, and 10). In lane 4, the effect of DTT alone was tested. Lanes 5, 7, and 9, show cells without DTT pretreatment. Nuclear extracts were prepared and analyzed for AP-1 activity by EMSA. (B) The influence of SL **2** on AP-1 DNA binding before incubation of DTT addition. Lane 1 shows untreated control cells. In lane 2, cells were treated with 100 ng/ml PMA alone for 1 h, in lane 3 for 4 h. In lanes 4, 6, 8, and 10 cells were stimulated with PMA for 1 h and subsequently incubated with different concentrations of SL **2**. Two hours after SL addition, DTT was added to a final concentration of 5 mM for 1 h (lanes 6, 8, and 10). In lanes 5, 7, and 9 cells were prestimulated with PMA for 1 h and subsequently incubated with SL **2** at the indicated concentrations for 3 h. Nuclear extracts were prepared and analyzed for AP-1 activity by EMSA. A filled arrowhead indicates the position of AP-1 DNA complexes. The open circle denotes a non-specific activity binding to the probe. The filled circle shows unbound oligonucleotide.

gold(I) salts and selenite by mutational analysis of cysteine residues in the DNA binding domain of Jun and Fos.[21] The sequence lysine-cysteine-arginine is also conserved in other members of the Jun and Fos families, making it highly likely that, in general, these proteins are targeted by alkylating compounds. Recently, Pérez-Sala et al.[22] could show that 15-deoxy-$\Delta^{12,14}$-prostaglandin J_2, which also possesses an α,β-unsaturated carbonyl group in the cyclopentenone ring, can react with cysteines in *c*-Jun proteins by Michael's addition.

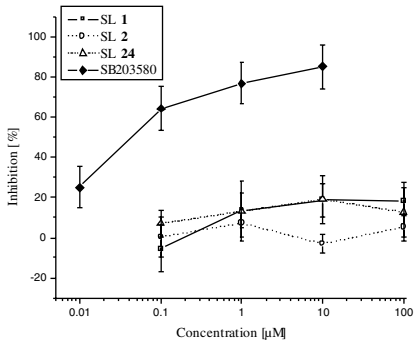

Figure 8. Results of p38 MAPK assay demonstrating the effects of SL **1**, **2**, and **24** on p38 enzyme activity. All compounds were tested in different concentrations ranging from 0.01 to 100 µM. SB203580 served as a reference and was able to block more than 50% of enzyme activity at 0.1 µM or higher. SL **1**, SL **2**, and SL **24** were found to leave p38 MAPK activity fairly unaffected at all concentrations tested.

Attachment of the cyclopentenone prostaglandin occurs at cysteine 269, which is located in the *c*-Jun DNA binding domain. Interestingly, it was also demonstrated that 15d-PGJ_2 can induce *c*-Jun dimerization through the formation of intermolecular disulfide bonds or 15d-PGJ_2-bonded dimers. Whether this latter mechanism may also be discussed for SLs has to be proven in future experiments.

2.5. SLs have no effect on p38 MAPK

To determine whether SLs affect the MAP kinase p38, three different SLs—parthenolide (**2**), 4β,15-epoxy-miller-9*E*-enolide (**1**), and 11α,13-dihydrohelenalin acetate (**24**)—as well as the p38-MAP kinase inhibitor SB203580 as a reference were tested in an ELISA according to Forrer et al.[24] In this assay, p38 MAPK phosphorylates ATF-2 and the amount of phosphorylated substrate reflects enzyme activity. Results are shown in Figure 8. Even at high concentrations SLs had no effect on p38 MAP kinase activity. This is in accordance with previous results which demonstrated that the SL parthenolide does not influence LPS-induced phosphorylation of p38 MAPK,[10] but prevents p38 MAPK activation by inhibiting the IL-1 receptor/TLR pathway at the level of MAPKKK or further upstream.[25]

3. Conclusion

The small molecules of SLs have been suggested to serve as lead compounds for the design of new antiinflammatory drugs.[9] Continuing our studies on QSAR of SLs and their antiinflammatory activity, we here present a QSAR study on their inhibitory activity of IL-8 production. Our data demonstrate again that the occurrence of an α-methylene-γ-lactone is the most important parameter for a strong inhibitory activity followed by LUMO2 which corresponds to the reactivity of the second reaction center of the SL. Concentrations necessary for a 50% inhibition correlate quite well with those necessary for a complete inhibition of NF-κB DNA binding. Moreover, a better

correlation coefficient was obtained from the QSAR analysis with IL-8 than using NF-κB DNA binding as target ($R = 0.821$ vs $R = 0.709$), demonstrating our improved QSAR studies by using IC_{50} values resulting from an ELISA. Despite the small data set there are good agreements over a wide range when comparing the experimental with the predicted IC_{50}-values for inhibition of IL-8 production (see Table 1 and Fig. 3 left). Nevertheless, it cannot be excluded that also the type of assay used, that means ELISA versus EMSA, may contribute to the improvement. Further parameters concerning bioavailability, for example, plasma protein binding as well as unwanted side effects such as allergenicity and cytotoxicity whose structural requirements unfortunately overlap with those of the antiinflammatory activity, have to be considered when creating a new lead structure to develop potent cytokine suppressing drugs.

Moreover, we proved that SLs inhibit DNA binding of the transcription factor NF-κB as well as of AP-1. These transcription factors are simultaneously necessary for the expression of IL-8. Therefore, SLs and those drugs that target both transcription factors may have profound effects on various diseases by affecting different sides in inflammatory processes. It was already shown that use of a potent NF-κB inhibitor resulted in a significant decrease in joint swelling in mice with collagen-induced arthritis, and that inhibition of AP-1 has beneficial effects on joint destruction.[26]

4. Experimental

4.1. Abbreviations

AP-1, activator protein-1; calcd: calculated; Cys, cysteine; 15d-PGJ_2, 15-deoxy-$\Delta^{12,14}$-prostaglandin J_2; DTT, dithiothreitol; EDTA, ethylenediaminetetraacetic acid; EGTA, ethylene glycol-bis(β-aminoethyl)*N*,*N*,*N*′*N*′tetraacetic acid; ELISA, enzyme-linked immunosorbent assay; EMSA, electrophoretic mobility shift assay; exp, experimental; FBS, fetal bovine serum; Hepes, (*N*-[2-hydroxyethyl] piperazine-*N*′-[2-ethanesulfonic acid]); IC_{50}, half-maximal inhibitory concentration; IC_{100}, inhibitory concentration; IL-8, interleukin-8; Mab, monoclonal antibody; MAPK, mitogen-activated protein kinase;

Table 2. List of the investigated SLs and their origin

No.	Name	Origin/reference
I.1 Germacrolides		
1	4β,15-Epoxy-miller-9*E*-enolide	*Milleria quinqueflora*[28]
2	Parthenolide	Sigma-Aldrich
3	3-Acetoxy-costunolide	*Podachaenium eminens*[29]
4	8α-Hydroxy-9β-tigloyloxy-germacra-4*E*,1(10)*E*-dien-6β,12-olide	*Montanoa hibiscifolia*[30]
5	8α-(2′,3′-Epoxy-2′-methylbutyryloxy)-1α-methoxy-9-oxo-10α*H*-germacra-4*E*-en-6β,12-olide	*M. hibiscifolia*[30]
I.2 Furanoheliangolides		
6	Budlein A	*Viguiera sylvatica*[31]
7	Niveusin A	*V. sylvatica*[31]
8	2β-Hydroxy-niveusin B	*V. sylvatica*[31]
9	Niveusin B	*V. sylvatica*[31]
10	4,5-Isobudlein A	*V. sylvatica*[31]
11	2β-Methoxy-2-deethoxy-phantomolin	*Elephantopus mollis*[32]
I.3 Melampolides		
12	Molephantin	*E. mollis*[32]
13	8α-(2′,3′-Epoxy-2′-methylbutyryloxy)-9-oxo-germacra-4*E*,1(10)*Z*-dien-6β,12-olide	*M. hibiscifolia*[30]
II. Eudesmanolides		
14	Isoalantolactone/alantolactone (3:1)	Sigma-Aldrich
15	1β-Acetoxy-4α-hydroxy-15-isobutyryloxy-eudesma-11(13)-en-12,8β-olide	*Mikania cordifolia*[33]
16	8α-(2′,3′-Epoxy-2′-methylbutyryloxy)-4α-hydroxy-9-oxo-5β*H*-eudesma-1*Z*,11(13)-dien-6β,12-olide	*M. hibiscifolia.*[30]
III. Guaianolides		
17	3,4-Epoxy-dehydroleucodine	*P. eminens*[29]
18	Dehydroleucodine	*P. eminens*[29]
19	3-Chloro-dehydroleucodine	*P. eminens*[29]
20	3-Oxo-guaia-1,4,11(13)-trien-12,8α-olide	*Decachaeta thieleana*[34]
21	Thieleanin	*D. thieleana*[a]
22	2-Oxo-guaia-1(5),11(13)-dien-12,8α-olide	*D. thieleana*[a]
IV. Pseudoguaianolides		
23	11,13-Dihydrohelenalin methacrylate	*Arnica montana*[35]
24	11,13-Dihydrohelenalin acetate	*A. montana*[35]
V. Standard		
25	Dexamethasone	Sigma-Aldrich

[a] Murillo, R.; Castro, V.; Garcia-Pineres, A. J.; Klaas, C. A.; Merfort, I., unpublished results.

NF-κB, nuclear factor-κB; NP-40, Nonidet P-40; PBS, phosphate-buffered saline; PMA, phorbol myristate acetate; PMSF, phenylmethylsulfonyl fluoride; Poly(dI-dC), polydeoxyinosinic-deoxycytidylic acid, double-stranded alternating co-polymer; QSAR, quantitative structure–activity relationship; rpm, rotations per minute; SL, sesquiterpene lactone; TNF-α, tumor necrosis factor alpha.

4.2. Test compounds

Sesquiterpene lactones were isolated from different plants (see Table 2), while isohelenin, parthenolide, and dexamethasone were purchased from Sigma. Stock solutions (10 and 100 mM) of the SLs and 1 mM stock solution of dexamethasone were prepared in DMSO (dimethylsulfoxide).

4.3. Cells

HeLa229 cells as well as Jurkat T-cells were maintained in RPMI 1640 (Gibco, Karlsruhe), supplemented with 10% fetal bovine serum (Sigma), 2 mM L-glutamine (Sigma), and 100 IU/ml penicillin and 100 μg/ml streptomycin (Roche Diagnostics, Mannheim). TNF-α was purchased from Roche Diagnostics and PMA was from Calbiochem (Bad Soden).

4.4. IL-8-ELISA

For IL-8 ELISA, HeLa229 cells were seeded at a density of 2.5×10^4 cells/well of a 24-well plate (Greiner, Frickenhausen, Germany) and allowed to attach overnight. On the next day cells were preincubated with the test compounds for 1 h and the IL-8 synthesis was stimulated by the addition of 2 ng/ml (800 U/ml) mouse TNF-α (Roche Diagnostics) for 24 h at 37 °C in a humified 5% CO_2 atmosphere. The amount of IL-8 secreted into the supernatant was determined by an ELISA with optimal concentrations of a mouse anti-human IL-8 monoclonal antibody (Mab) (Pharmingen, San Diego, USA) and a biotinylated mouse anti-human IL-8 Mab (Pharmingen) as detecting body. 96-well Maxisorp immunoplates (Nunc, Roshilde, Denmark) were coated overnight with anti-human IL-8 Mab at 4 °C. After non-specific binding sites were blocked with blocking buffer (10% FBS in PBS, pH 7.4) for 2 h at room temperature, supernatants and standards were added to the wells and incubated overnight at 4 °C. Plates were washed four times between all steps with 0.05% Tween 20 in PBS, pH 7.4. After sample incubation, biotin-labeled anti-human Mab was added and plates were incubated for 1 h. Finally, an avidin–biotin–alkaline phosphatase complex (StreptABC-AP kit; Dako, Glostrup, Denmark) was added for 1 h at 37 °C. For signal development the wells were incubated with *p*-nitrophenylphosphate disodium (pNPP; Sigma-Aldrich) for 20 min at 37 °C and the OD (optical density) was determined at wavelengths 405 and 490 nm. IL-8 concentrations were calculated from the straight-line portion of a standard curve using recombinant human IL-8 (Pharmingen).[27]

Cell viability after 24 h continuous exposure to SLs was measured by the trypan blue method. Percent cell viability was calculated as: number of viable cells/total cell number × 100.

4.5. Preparation of total cell extracts

Total protein extracts were prepared from Jurkat T-cells and HeLa229 cells using a high-salt detergent buffer (Totex: 20 mM Hepes, pH 7.9, 350 mM NaCl, 20% (v/v) glycerol, 1% (v/v) Nonidet P-40 (NP-40), 1 mM $MgCl_2$, 0.5 mM EDTA, 0.1 mM EGTA, 1.0 mM DTT, 0.0005% PMSF, and 1% aprotinin-solution). Cells were harvested by centrifugation, HeLa cells were pretreated with trypsin, washed once in ice-cold phosphate-buffered saline (PBS), and resuspended in 50 μl Totex buffer. The cell lysate was incubated on ice for 30 min and then centrifuged for 5 min at 13,000 rpm and 4 °C. The lysates were stored at −80 °C until used for EMSA.

4.6. Preparation of nuclear protein extracts

HeLa229 cells were washed with PBS in the wells. Two milliliters of ice-cold buffer A (10 mM Hepes, pH 7.6, 15 mM KCl, 2 mM $MgCl_2$, and 0.1 mM EDTA) was added and incubated for 10 min on ice. The buffer was removed, and after addition of 1 ml of Igepal (buffer A + 0.2% NP-40, 1 mM DTT, 1% aprotinin solution, and 0.0005% PMSF) the cells were incubated for further 5 min on ice. The cells were harvested and centrifuged for 10 min at 4500 rpm and 4 °C. Remaining nuclei in the wells were scrapped off in 100 μl buffer C (25 mM Hepes, 50 mM KCl, 0.1 mM EDTA, 10% glycerol, 1 mM DTT, 0.0005% PMSF, and 1% aprotinin-solution) and combined to the pellets. To lyse the nuclear membrane, 8.5 μl of 5 M NaCl was added and the lysate was mixed for 30 min at 4 °C and 550 rpm. After centrifugation for 10 min at 4 °C and 1300 rpm, the nuclear protein extracts were stored at −80 °C until used for EMSA.

4.7. Electrophoretic mobility shift assay

Protein extracts were prepared as mentioned above. The protein content of the extract was determined and equal amounts of protein (10–20 μg) were added to a reaction mixture containing 20 μg bovine serum albumin (BSA) (Sigma), 2 μg poly(dI-dC) (Roche Molecular Biochemicals), 2 μl buffer D + (20 mM Hepes, pH 7.9, 20% glycerol, 100 mM KCl, 0.5 mM EDTA, 0.25% NP-40, 2 mM DTT, and 0.1% PMSF), 4 μl buffer F (20% Ficoll 400, 100 mM Hepes, 300 mM KCl, 10 mM DTT, and 0.1% PMSF), and 100,000 cpm (Cerenkov) of a P^{32}- or P^{33}-labeled oligonucleotide for NF-κB or AP-1 made up to a final volume of 20 μl with distilled water. Samples were incubated at room temperature for 25 min. NF-κB oligonucleotide (5′-AGT TGA GGG GAC TTT CCC AGG C-3′, Promega) or AP-1 oligonucleotide (5′-GAG GTG AGG GCC TTC CCT TAG-3′, Promega) was labeled using [γ^{33}P]dATP (3000 Ci/mmol; Amersham Pharmacia Biotech) or [γ^{32}P]dATP (3000 Ci/mmol; Amersham Pharmacia Biotech) and a T4 polynucleotide kinase (New England Biolabs). The probes were resolved through non-denaturing 4% polyacrylamide gel electrophoresis.

4.8. RNA isolation and reverse transcription (RT)

RNA was extracted using the RNeasy® Mini Kit (Qiagen, Hilden, Germany). For reverse transcription, 1.75 μg total RNA was adjusted to a volume of 8 μl. One microliter of random hexamers (50 ng/μl) and 1 μl dNTP mix (10 mM) were added. The mixture was denatured at 70 °C for 10 min and chilled on ice. cDNA synthesis was made by adding a mixture containing RT buffer (200 mM Tris–HCl, pH 8.4, 500 mM KCl), DTT, $MgCl_2$, RNase OUT, and Superscript II™ RT. The final concentration of these reagents was 20, 50, 0.1, 5 mM, and 2 U/50 μl and 2.5 U/50 μl, respectively. The samples were incubated at room temperature for 10 min, at 42 °C for 50 min, and at 70 °C for 15 min. One microliter of RNase H (2 U/μl) was added per reaction followed by incubation at 37 °C for 20 min. The cDNA solution was subsequently diluted to 100 μl in DEPC-treated water and stored at −80 °C.

4.9. Quantitative RT-PCR

In a 50 μl PCR, 3 μl cDNA (corresponding to 30–50 ng total RNA input) was amplified in a 7700 Sequence Detector, using the 2× Universal Master Mix, 50 nM primers, and 100 nM probe (VIC-TAMRA-labeled) for the 18S rRNA internal control, and 300 nM primers and 100 nM probe (FAM-TAMRA-labeled) for the IL-8 gene. Primers and probe sets were designed with the Primer Express™ software. The cycle number at which the fluorescence exceeded the threshold of detection (C_T) for ribosomal RNA was subtracted from that of the target genes for each well (ΔC_T). Messenger RNA levels were then indicated as $2^{-\Delta\Delta C_T}$ where $\Delta\Delta C_T$ returns to the ΔC_T of unstimulated minus treated cells.

Sequences of primers and probes for the TaqMan®-analysis:

Gene: Human interleukin-8 (hIL-8)
Primer sequences:
Forward: 5′-ACTGACATCTAAGTTCTTTAGCACT CC-3′
Reverse: 5′-GCCTTCCTGATTTCTGCAGC-3′
Probe: 5′-TGGCAAAACTGCACCTTCACACAG-3.

4.10. p38 MAPK assay

The activity was measured using the method of Forrer et al.[24] Microtiter plates were coated with 50 μl ATF-2-solution (Upstate Biotechnologies; 10 μg/ml) for 1.5 h at 37 °C. After three times washing with bidestilled water, plates were incubated with blocking buffer (50 mM Tris, 0.05% Tween 20, and 0.25% BSA) for 30 min. Thereafter the plates were washed three times and 50 μl kinase mixture (50 mM Tris–HCl, 10 mM $MgCl_2$, 10 mM β-glycerol phosphate, 100 μg/ml BSA, 1 mM DTT, 100 μM ATP, 100 μM Na_3VO_4, and 10 ng p38α-activated) with or without different inhibitor concentrations was added to the wells and incubated for 1 h at 37 °C. After three washes, plates were incubated with a rabbit anti-phospho-ATF-2 antibody (New England Biolabs; 1:2000) for 1 h at 37 °C and washed again three times. Then alkaline phosphatase-labeled anti-rabbit IgG antibody (SantaCruz Biotechnology; 1:2000) was added for 1 h at 37 °C followed by a three times washing. Subsequently, 100 μl alkaline phosphatase substrate solution (3 mM 4-nitrophenylphosphate, and 50 mM $NaHCO_3$, 50 mM $MgCl_2$, 100 μl/well) was added to each well for 1.5 h at 37 °C. The formation of 4-nitrophenolate was measured at 405 nm using a microtiter plate reader.

4.11. Statistical analysis

Statistical analysis was performed by using the Origin 7.0 software. Data are reported as means ± SD and analyzed using an independent *t*-test (two groups). A p value <0.05 is considered statistically significant. $*p < 0.05$, $**p < 0.005$ versus positive control.

4.12. QSAR calculations

Descriptor calculation. Three-dimensional structures of the molecules were created using the molecular modeling package HyperchemPro® (Version 6.02). Energy minimizations were performed with the force field MM+ using the Polak–Ribière minimization algorithm. Low-energy conformations of the SLs were created using the conformational search option. The starting structures were initially minimized to an RMS (root mean square) gradient <0.01 kcal mol^{-1} $Å^{-1}$. All rotatable cyclic bonds were included as variable torsions and allowed to be changed simultaneously. The search was performed applying a usage-directed search method and standard settings for duplication test. A search run was terminated after energy minimization of 2500 unique starting geometries. Acyl side chains were not included in the conformational search. They were added manually to the SL-conformer with the lowest energy and the resulting models were energy minimized to an rms-gradient as described above. The final geometries were obtained with the semi-empirical AM1 method. The resulting geometries were transferred to the software CAChe® (Fujitsu Inc.), which can calculate constitutional, topological, electrostatic, and quantum chemical descriptors. Constitutional descriptors are related to the number of atoms, bonds, and functional groups in each molecule. Topological descriptors, like the shape and connectivity indices, include valence and non-valence molecular connectivity indices calculated from the hydrogen suppressed formula of the molecule, encoding about the size, composition, and the degree of branching in the molecule. The quantum chemical descriptors include information about the molecular orbital energy levels. For all calculated descriptors and their abbreviations used in the following calculations, see Table 3.

4.12.1. Model selection by means of multiple linear regression. After calculation of the descriptors, an intercorrelation analysis of the descriptors was performed. During the regression analysis equations containing variables with an intercorrelation coefficient >0.85 were discarded. Selection of relevant descriptors was performed using the SAS.6.12® Procedure REG (SAS Institute Inc., Cary, NC, USA; REG = multiple linear

Table 3. The calculated descriptors and the abbreviations used for the QSAR calculations

Structural descriptors	Abbreviation
Total number of α,β-unsaturated carbonyl structures in the molecule (sum of ML, ENON, and ACYL)	UNC
α-Methylene-γ-lactone	ML
Conjugated ester groups	UNA
Conjugated keto or aldehyde functions	ENONE
Number of oxygen atoms	ATOM
Number of hydroxyl groups	OH
Position of the O-function in relation to the α-methylene-γ-lactone	O-POS
The octanol water partition coefficient	LOG *P*
Electron affinity	EA
Dipole moment	DIPOL
Molar refractivity	MR
Connectivity indices	CN0-2
Shape indices	SH1-3
Highest occupied molecular orbital	HOMO
Lowest unoccupied molecular orbitals	LUMO1-3

regression). However, we did not make use of one of the built-in selection criteria like 'forward' or 'backward' but proceeded in two steps: in the first step, the linear models with up to five descriptors were listed which yielded the highest R^2 (selection criterion 'R^2' as a measure of explained variation). In the second step, beginning with the best model with five descriptors, non-significant parameters were discarded until every parameter in the model contributed significantly to the model fit.

Acknowledgment

We gratefully acknowledge the financial support of the Volkswagen-Stiftung. M.T.L. thanks funding by the Landesgraduiertenförderung Baden-Württemberg. We are grateful to Mrs. K. Bauer, Pharmaceutical Chemistry, University of Tübingen, Germany, for technical support and to Dr. G. Grassl, Institut of Medizinische Mikrobiologie und Krankenhaushygiene, Universitätsklinikum Tübingen, Germany, for valuable scientific advice and to Dr. J. Schwager, DSM Nutritional Products, Kaiseraugst, Switzerland, for the support in carrying out the Taqman® analyses.

References and notes

1. Baggiolini, M.; Dewald, B.; Moser, B. *Adv. Immunol.* **1994**, *55*, 97–179.
2. Wuyts, A.; Proost, P.; Van Damme, J. *The Cytokine Handbook*, 3rd ed.; Academic Press: San Diego, 1998, Chapter 10, pp 271–311.
3. Hoffmann, E.; Dittrich-Breiholz, O.; Holtmann, H.; Kracht, M. *J. Leukocyte Biol.* **2002**, *72*, 847–855.
4. Roebuck, K. A. *J. Interferon Cytokine Res.* **1999**, *19*, 429–438.
5. Karin, M.; Ben Neriah, Y. *Annu. Rev. Immunol.* **2000**, *18*, 621–663.
6. Schulte, R.; Grassl, G. A.; Preger, S.; Fessele, S.; Jacobi, C. A.; Schaller, M.; Nelson, P. J.; Autenrieth, I. B. *FASEB J.* **2000**, *14*, 1471–1484.
7. Shaulian, E.; Karin, M. *Oncogene* **2001**, *20*, 2390–2400.
8. Winzen, R.; Kracht, M.; Ritter, B.; Wilhelm, A.; Chen, C. Y.; Shyu, A. B.; Muller, M.; Gaestel, M.; Resch, K.; Holtmann, H. *EMBO J.* **1999**, *18*, 4969–4980.
9. Siedle, B.; Garcia-Pineres, A. J.; Murillo, R.; Schulte-Monting, J.; Castro, V.; Rungeler, P.; Klaas, C. A.; Da Costa, F. B.; Kisiel, W.; Merfort, I. *J. Med. Chem.* **2004**, *47*, 6042–6054.
10. Hehner, S. P.; Hofmann, T. G.; Droge, W.; Schmitz, M. L. *J. Immunol.* **1999**, *163*, 5617–5623.
11. Lyss, G.; Schmidt, T. J.; Merfort, I.; Pahl, H. L. *Biol. Chem.* **1997**, *378*, 951–961.
12. Mazor, R. L.; Menendez, I. Y.; Ryan, M. A.; Fiedler, M. A.; Wong, H. R. *Cytokine* **2000**, *12*, 239–245.
13. Garcia-Pineres, A. J.; Castro, V.; Mora, G.; Schmidt, T. J.; Strunck, E.; Pahl, H. L.; Merfort, I. *J. Biol. Chem.* **2001**, *276*, 39713–39720.
14. Hall, I. H.; Lee, K. H.; Starnes, C. O.; Sumida, Y.; Wu, R. Y.; Waddell, T. G.; Cochran, J. W.; Gerhart, K. G. *J. Pharm. Sci.* **1979**, *68*, 537–541.
15. Rüngeler, P.; Castro, V.; Mora, G.; Goren, N.; Vichnewski, W.; Pahl, H. L.; Merfort, I.; Schmidt, T. J. *Bioorg. Med. Chem.* **1999**, *7*, 2343–2352.
16. Schmidt, T. J. *Pharm. Pharmacol. Lett.* **1999**, *9*, 9–13.
17. Godwin, A. K.; Meister, A.; O'Dwyer, P. J.; Huang, C. S.; Hamilton, T. C.; Anderson, M. E. *Proc. Natl. Acad. Sci. U.S.A.* **1992**, *89*, 3070–3074.
18. Schmidt, T. J. *Bioorg. Med. Chem.* **1997**, *5*, 645–653.
19. Bork, P. M.; Schmitz, M. L.; Kuhnt, M.; Escher, C.; Heinrich, M. *FEBS Lett.* **1997**, *402*, 85–90.
20. Kang, J. S.; Yoon, Y. D.; Lee, K. H.; Park, S. K.; Kim, H. M. *Biochem. Biophys. Res. Commun.* **2004**, *313*, 171–177.
21. Handel, M. L.; Watts, C. K.; deFazio, A.; Day, R. O.; Sutherland, R. L. *Proc. Natl. Acad. Sci. U.S.A.* **1995**, *92*, 4497–4501.
22. Perez-Sala, D.; Cernuda-Morollon, E.; Canada, F. J. *J. Biol. Chem.* **2003**, *278*, 51251–51260.
23. Klatt, P.; Molina, E. P.; De Lacoba, M. G.; Padilla, C. A.; Martinez-Galesteo, E.; Barcena, J. A.; Lamas, S. *FASEB J.* **1999**, *13*, 1481–1490.
24. Forrer, P.; Tamaskovic, R.; Jaussi, R. *Biol. Chem.* **1998**, *379*, 1101–1111.
25. Uchi, H.; Arrighi, J. F.; Aubry, J. P.; Furue, M.; Hauser, C. *J. Allergy Clin. Immunol.* **2002**, *110*, 269–276.
26. Tak, P. P.; Gerlag, D. M.; Aupperle, K. R.; van de Geest, D. A.; Overbeek, M.; Bennett, B. L.; Boyle, D. L.; Manning, A. M.; Firestein, G. S. *Arthritis Rheum.* **2001**, *44*, 1897–1907.
27. Schulte, R.; Autenrieth, I. B. *Infect. Immun.* **1998**, *66*, 1216–1224.
28. Castro, V.; Rungeler, P.; Murillo, R.; Hernandez, E.; Mora, G.; Pahl, H. L.; Merfort, I. *Phytochemistry* **2000**, *53*, 257–263.
29. Castro, V.; Murillo, R.; Klaas, C. A.; Meunier, C.; Mora, G.; Pahl, H. L.; Merfort, I. *Planta Med.* **2000**, *66*, 591–595.
30. Müller, S.; Murillo, R.; Castro, V.; Brecht, V.; Merfort, I. *J. Nat. Prod.* **2004**, *67*, 622–630.
31. Tamayo-Castillo, G.; Jakupovic, J.; Bohlmann, F.; Castro, V. *Phytochemistry* **1989**, *28*, 2737–2740.
32. Banerjee, S.; Schmeda-Hirschmann, G.; Castro, V.; Schuster, A.; Jakupovic, J.; Bohlmann, F. *Planta Med.* **1986**, 29–32.
33. Klaas C.A. Thesis, Albert-Ludwigs-Universität Freiburg, 2001.
34. Castro, V.; Ciccio, F.; Alvarado, S.; Bohlmann, F.; Schmeda-Hirschmann, G. *Liebigs Ann. Chem.* **1983**, 974–981.
35. Klaas, C. A.; Wagner, G.; Laufer, S.; Sosa, S.; Della Loggia, R.; Bomme, U.; Pahl, H. L.; Merfort, I. *Planta Med.* **2002**, *68*, 385–391.